Tunable magnetic anisotropy in epitaxial GaMnAs films: Evidence of temperature control

M. Dehbaoui[1,2], S. Kamara[1], Q. H. Tran[1*], J. Sadowski[3,4], J. Z. Domagala[4], A. Boukra[5], R. Dumas[1], S. Charar[1], F. Terki[1*]

[1]*Institut Charles Gerhardt Montpellier, UMR 5253 CNRS-UM, Place Eugene Bataillon, 34095 Montpellier, France*
[2]*Laboratoire de Mécanique, Physique et Modélisation Mathématique, Université Dr. Yahia Fares, 26000 Médéa, Algérie*
[3]*MAX-IV Laboratory, Lund University, P.O. Box 118, SE-221 00 Lund, Sweden*
[4]*Institute of Physics, Polish Academy of Sciences, al. Lotników 32/46, PL-02-668 Warsaw, Poland*
[5]*University of Mostaganem, Avenue Hamadou Hossine, Mostaganem, Algeria*

*Corresponding authors: E-mail: quang-hung.tran@umontpellier.fr; ferial.terki@umontpellier.fr

Abstract

The magnetic field dependencies of Hall resistance are studied for $Ga_{0.94}Mn_{0.06}As/In_{0.15}Ga_{0.85}As$ film. The Hall resistance shows a slanted hysteresis cycle, emphasizing the existence of both in-plane and out-of-plane magnetization components. The anisotropy constants of the sample with out-of-plane magnetization are extracted from the angular dependence of Hall resistance measurements. The angular dependence of free magneto-crystalline energy theoretical analysis allows us to confirm the dominance of uniaxial magnetic anisotropy at specific temperatures. Here, precise angular dependence of magnetoresistance Hall Effect measurements and careful analysis using free energy model, enable us to demonstrate how the magnetic easy axis could be reoriented by the temperature within the ferromagnetic phase at the temperature far from the Curie Weiss value. This promising property will offer applicative opportunity of GaMnAs material with temperature induced transition of easy magnetization axis in detection of weak magnetic fields within the cryogenic range of low temperature phenomenon. Copyright © 2017 VBRI Press.

Keywords: Diluted magnetic semiconductor materials, spintronics, hall resistance, magnetic anisotropy.

Introduction

Dilute magnetic semiconductors (DMS) are interested in advanced research to find out new materials for magneto-electronic (spintronic) devices, because this materials offers to manipulate both charge and spin properties of the charge carriers. The GaMnAs epitaxial thin film is one of desired DMS materials. Since they are based on galium arsenide – one of semiconductors widely used for optoelectronic devices, one may foresee the spintronics devices based on GaMnAs to be eligible for applications with easily accessible temperatures. Currently, GaMnAs films are developed with relatively high Curie temperature (T_C ~185K [1], T_C ~ 200 K [2]) which makes them promising for applications. However the magnetic anisotropy and magnetization reversal mechanisms in GaMnAs-based structures are still under investigation. These properties depend on parameters such as hole concentration, temperature and growth-induced strain [3, 4] *i.e.*, the magnetic properties of the layers could be predefined by the selection of these parameters.

As investigated theoretically [5] and experimentally [6, 7], the magnetic anisotropy of GaMnAs can be efficiently controlled by epitaxial strain. In the case of GaAs based ternary alloy, such as GaMnAs, the strain state of the thin epitaxial layers can be easily defined by the use of a thick, relaxed InGaAs buffer layer deposited on GaAs substrate. Instead of InGaAs one may use also other GaAs-based ternary (or multinary) alloys such as GaAsSb, GaAsP, GaAsBi, but ternary InGaAs buffers are the easiest choice in terms of the MBE growth conditions and possible *in-situ* composition control (by RHEED oscillations [8, 9]). The percentage of Indium content in relaxed InGaAs buffer layer has a direct effect on the GaMnAs diluted semiconductor materials with the lattice mismatch, the so-called epitaxial strain.

With a tensile strain control of $In_yGa_{1-y}As(100)$ under layer, the magnetization of $Ga_{1-x}Mn_xAs$ layer is in-plane with low composition of Mn (low concentration of holes), and the magnetization is in out-of-plane configuration with high composition of Mn [10, 11]. In contrast for a compressive strain control by an underlayer *i.e.*, GaAs, the magnetization of $Ga_{1-x}Mn_xAs$ layer is confined in-plane with high concentration of holes [3, 5, 7, 12] and out-of plane with low concentration of holes. Moreover, the in-plane easy magnetization axis of the very thin GaMnAs layers [13] can be rotated within the thin film plane by adjusting the concentration of holes (via voltage applied to gate electrodes).

However, the much more application-significant dedicated with changing of magnetization direction from in-plane to out-of-plane orientation of GaMnAs thin film has not been demonstrated yet, neither for GaMnAs layers under compressive strain, nor under tensile strain. In this paper, we study the magnetization along the main crystallographic directions of $Ga_{0.94}Mn_{0.06}As/In_{0.15}Ga_{0.85}As$ samples through Hall Effect measurements. Our aim is to understand and then control the in-plane and out-of-plane magnetization with temperature using the Hall Effect characterization. The Curie temperature of the sample was estimated from the maximum of the resistivity curves, corresponding to $d\rho/dT = 0$ (**Fig. 1**).
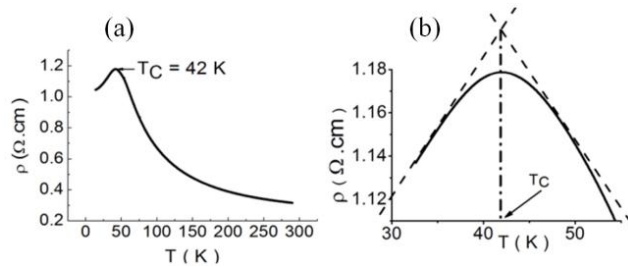

Fig. 1. (a) Resistivity *vs.* temperature of the investigated sample. (b) Method to determine Currie temperature (T_C).

Experimental

The $Ga_{1-x}Mn_xAs$ layers were growth by a molecular beam epitaxy at 230 °C on a semi-insulating GaAs(001) substrates using the KRYOVAK MBE system at MAX-Lab, Lund University, Sweden [**14**, **15**]. The growth was performed with As_2 flux generated from an arsenic valve cracker source. The GaAs(001) substrate (1.5×1.5 cm) were glued by Indium to the molybdenum holder. After loading into the MBE growth chamber, the substrates were thermally dehydrated by heating the holder to 590 °C under As_2 flux. Then $GaAs/Ga_{0.85}In_{0.15}As$ buffer layers were growth at the optimized conditions *i.e.*, substrate temperature of 590 °C for growing GaAs layer and 480 °C for growing InGaAs layer; As_2/Ga flux ratio is about 5. The quality of InGaAs epitaxial layer was determined by *in-situ* X-ray diffraction using reciprocal space mapping around asymmetrical 224 reciprocal lattice points. Then the substrate temperature was lowered down to 230 °C, and stabilized for half an hour before the growth of $Ga_{0.94}Mn_{0.06}As$ (1000 nm) layer (As/Ga ratio of about 1.5, the growth rate of 0.2 monolayer/s). Both Ga and As_2 impinging fluxes were well measured by RHEED oscillations for GaAs growth [**15-17**].

The devices were patterned into the Hall bar of 50 μm width and 2mm length by photolithography and wet chemical etching. The bars are aligned along [110] crystallographic direction. The contact pads are made of ZnAu layer (500×500 μm^2, 300 nm) for ohmic contacts using a sputtering deposition, and using photolithographic lift-off method. Transport properties measurements were carried out under precise controlled temperature of an in-house cryostat. The temperature of the cryostat could be well controlled from T = 5 K to 300 K. During the Hall measurements, a DC field was applied along the [110]

crystallographic direction aligned to the current polarization axis. The Hall voltage was measured in a transverse direction with the crystallographic direction, as shown in **Fig. 2a**. To ensure the uniformity of magnetization of the films, a DC magnetic field of 0.5 T was applied prior each measurement.
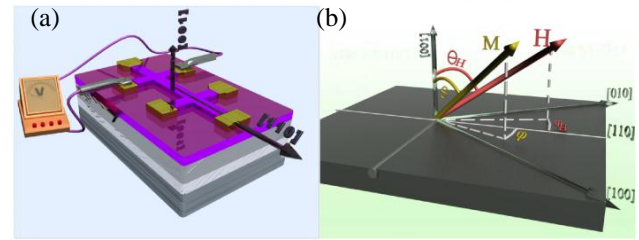

Fig. 2. (a) Scheme of a Hall bar pattern, the current is polarized and flows along the [110] direction. The four lateral pads indicate voltage contacts for both longitudinal R_{xx} and Hall resistance R_{xy} measurements. (b) Coordinate systems (θ_H, φ_H) and (θ, φ) are corresponding to the orientations of the magnetic field H and the magnetization M.

For theoretical calculation, the value of anisotropy constant was estimated as the arithmetic mean among a set of fitting results, the absolute uncertainty ΔK was estimated in function of the standard deviation (σ) of a series of *n* measurements as:

$$\Delta K = \frac{\sigma}{\sqrt{n}} = \sqrt{\frac{\sum_{j=1}^{n}(K_j - \overline{K})^2}{n(n-1)}}$$

. Where K_j is the result of the jth fit and $\overline{K}$ is the arithmetic mean of the considered n results.

Results and discussion

Hall effect measurement: When a current-carrying ferromagnetic semiconductor is placed in a magnetic field, the charge carriers, in the sample, are submitted to the Lorentz force perpendicular to both magnetic field and the current. At equilibrium, a Hall voltage appears at the semiconductor edges, and a corresponding resistance is measured [**18-24**].

$$R_H = \frac{R_0}{d}H\cos\theta_H + \frac{R_S}{d}M\cos\theta + \frac{k}{d}(M\sin\theta)^2\sin 2\varphi \quad (1)$$

In equation (1), first term is the ordinary Hall resistance. R_0 is the ordinary Hall coefficient. $H\cos\theta_H$ is the magnetic field's component perpendicular to the current direction. The second term is the anomalous Hall resistance arising from the asymmetric scattering of the conduction electrons from the magnetic moments in the sample; it is proportional to the component of the magnetization perpendicular to the current. R_S is the spontaneous Hall coefficient. The third term is Planar Hall resistance. In this term, the constant k is related to the difference in resistivity between the directions parallel to and perpendicular to the current. If there is an in-plane component ($M\sin\theta$) then, because of the magnetoresistance, the equipotential may not be perpendicular to the current, and a Hall-like voltage is generated [**25**].

The anomalous Hall resistance (Eq.1) is an odd function of M, whereas the planar Hall resistance is an even function of M. Consequently we can extract these components separately by subtracting (or adding) from the experimental curves of R_H. **Fig. 3** shows the Hall resistance as a function of magnetic field of the investigated sample $Ga_{0.94}Mn_{0.06}As/In_{0.15}Ga_{0.85}As$, in the ferromagnetic phase at T = 5 K. The data plotted in **Figs. 3a,b** and **Figs. 3c,d** are the measured Hall resistance and extracted planar Hall resistance when the magnetic field applied out-of-plane ($\theta_H = 0°$) and in-plane ($\theta_H = 90°$ and $\varphi_H = 0°$) to the samples. The Hall measurements were carried out with the magnetic fields applied normal to the sample plane. The slanted R_H curve (**Fig. 3a**) indicating that the in-plane component of magnetization is dominated for the $Ga_{0.94}Mn_{0.06}As$ layer, even with the presence of the buffer layer $In_{0.15}Ga_{0.85}As$. This is in good agreement with previous results studied by Kim *et al* [**26**]. The strong in-plane anisotropy of the sample is also confirmed by the two-step switching behaviour when the magnetic field is applied in-plane, as shown in **Fig. 3c**. In summary for the sample at 5 K, in-plane magnetic anisotropy is dominated.

We further investigate magnetic anisotropy at higher temperatures (20 K and 40 K). The R_H curves at 20 K are more square-like shape (**Fig. 3e**), and when the temperature is further increased, reaching the fluctuation zone near T_C (42 K), the R_H curves are closer to square shapes (**Fig. 3f**). This data set allows us to confirm that the out-of-plane magnetization component in the investigated sample is increased with the temperature. The same results were observed for sample with Indium concentration in the buffer layer close to 20 % [**27**]. Furthermore, there is a significant increasing in the coercive field (H_c) with the increment of θ_H. H_c increases from 50 Oe to 210 Oe for θ_H increasing from 0° to 90°. In other words, the out-of-plane magnetization component is easier to rotate than the in-plane magnetization component. These results confirm that the magnetic anisotropy of the sample is tunable by controlling the temperature.

Analysis of magnetic anisotropy

The magnetization behaviour of the sample can be described using the free energy formula given by [**28**].

$$F = -MH\left[\cos\theta\cos\theta_H + \sin\theta\sin\theta_H\cos(\varphi - \varphi_H)\right] + \left[2\pi M^2\cos^2\theta\right]$$

$$-\frac{M}{2}\left[\begin{array}{c} H_{2\perp}\cos^2\theta + H_{2//}\sin^2\theta\sin^2\varphi \\ + \frac{1}{2}H_{4\perp}\cos^4\theta + \frac{1}{4}H_{4//}\sin^4\theta\cos^2(2\varphi) \end{array}\right] \quad (2)$$

The first term is the Zeeman energy; the second term is the demagnetizing energy (shape anisotropy); and the third term is the energy due to the uniaxial and cubic anisotropies. $H_{2\perp}$ ($H_{2//}$) and $H_{4\perp}$ ($H_{4//}$) represent the perpendicular (planar) uniaxial and cubic anisotropy constants, respectively. θ_H, φ_H, θ and φ represent respectively the orientation of magnetic field and magnetization as depicted in **Fig. 2b**. The in-plane field
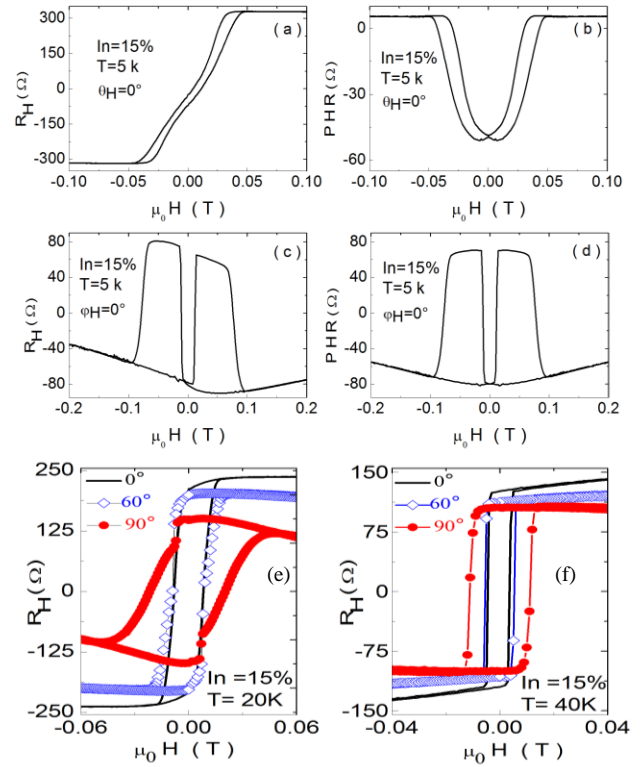
Fig. 3. The measured R_H at T = 5 K and extracted planar Hall resistance for the measurement with external field applied in the out-of-plane direction (a) and (b) and for the measurement with the external field applied in-plane of the sample (c) and (d). Hall resistance measurement as function of magnetic field with the field orientation from in-plane ($\theta_H = 90°$) to out-of-plane ($\theta_H = 0°$) at T = 20 K and T = 40 K (e) - (f).

anisotropy ($H_{2//}$) reflects the fact that in a zinc blende structure the directions [110] and [1$\bar{1}$0] are not equivalent [**29**].

Since the magnetization follows the position of the minimum magnetic energy, the equilibrium condition for any given field orientation can be obtained from equation (2) by minimizing the free energy with respect to θ and φ. The anisotropic field components can be independently determined from the angular dependence of the Hall measurements performed within either (001) or (110) plane (**Figs. 4** and **5**).
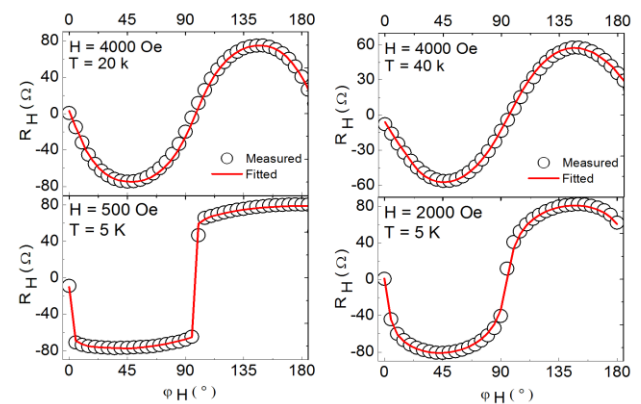
Fig. 4. Angular dependence of the measured Hall resistance (Open circle) for different fields applied in-plane of the sample at 5 K, 20 K and 40 K. The solid lines are the fitting results using Equations (3) and (4).

To determine in-plane component of anisotropy fields, we have performed planar Hall resistance measurements within (001) plane where ($\theta = \theta_H = \pi/2$). Then equation (2) can be written as:

$$F = -\frac{M}{2}[2H\cos(\varphi - \varphi_H) - H_{2//}\sin^2\varphi - \frac{1}{4}H_{4//}\cos^2(2\varphi)]$$

(3)

In this case, the Hall resistance takes the form:

$$R_H = \frac{k}{d}M^2\sin 2\varphi$$

(4)

The zero torque condition for the equilibrium implies $\partial F/\partial\varphi = 0$, the stability is given by the second derivative condition $\partial^2 F/\partial\varphi^2 > 0$.

Fitting the experimental data with respect to $H_{4//}$ and $H_{2//}$ in **Fig. 4** yields the values of in-plane anisotropy depicted in **Table 1**. The in-plane cubic anisotropy field of $H_{4//} = 1100 \pm 50$ Oe is the largest value at 5 K, where $H_{2//} = 400 \pm 50$ Oe. This indicates the dominance of cubic magnetic anisotropy and therefore the easy axes lie in the plane at low temperature, which confirms the result found in the configuration of classic Hall measurement.

The out-of-plane components of the anisotropy fields can be studied by performing Hall resistance measurements within the (110) plane where ($\varphi = \varphi_H = \pi/2$). The Hall resistance can be simplified to the equation:

$$R_H = \frac{R_0}{d}H\cos\theta_H + \frac{R_S}{d}M\cos\theta$$

(5)

Then, equation (2) becomes function of only θ and θ_H as following:

$$F = -\frac{M}{2}[(H_{2\perp} - 4\pi M)\cos^2\theta + \frac{1}{2}H_{4\perp}\cos^4\theta + 2H\cos(\theta - \theta_H)...$$

$$+ H_{2//}\sin^2\theta + \frac{1}{4}H_{4//}\sin^4\theta]$$

(6)

The conditions for the energy minima and stability should satisfy $\partial F/\partial\theta = 0$ and $\partial^2 F/\partial\theta^2 > 0$.

The data plotted with open circles in **Fig. 5** can be fitted with equation (5) and (6), using $4\pi M_{eff} = 4\pi M$; $H_{2\perp}$ and $H_{4\perp}$ as fitting parameters.
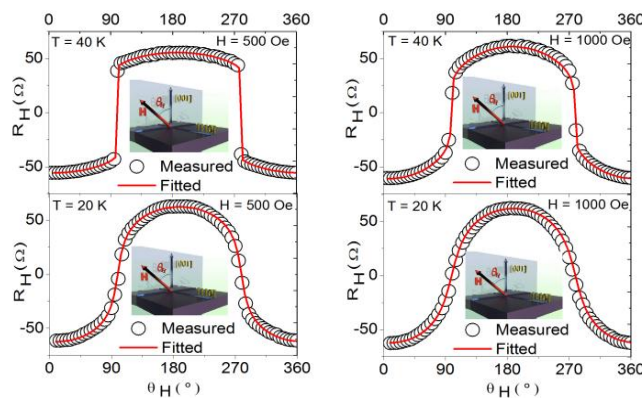

Fig. 5. Angular dependence of measured Hall resistance (Open circle) for the field applied out-of-plane direction (500 Oe and 1000 Oe) at 20 K and 40 K. The solid lines are the fitting results using Equations (5) and (6). Insets show the measurement configuration.

Table 1. Anisotropy fields analysis from the calculation. For all calculations $\Delta H = 50$ Oe.

T (K)	$H_{4//}$ (Oe)	$H_{2//}$ (Oe)	$H_{4\perp}$ (Oe)	$4\pi M_{eff}$ (Oe)
5	1100	400	-	-
20	450	300	-200	-1200
40	400	300	-200	-1400

The best fitting parameters values for $Ga_{0.94}Mn_{0.06}As/In_{0.15}Ga_{0.85}As$ film were obtained in the ferromagnetic phase. The results reveal a net dominance of the uniaxial anisotropy field ($H_{2\perp} = 4\pi M - 4\pi M_{eff}$) at 20 K and 40 K, indicating that at these temperatures, the magnetic easy axes lie along with the out-of-plane direction.

The preference for the magnetization to lay in particular direction can be illustrated by comparing the values of the magnetic free energy in the different crystallographic directions. Using the obtained values of the anisotropy fields, we have represented the angular dependence of the free magnetic energy in a polar plot in **Fig. 6**. We observed that the minimal energies occur in the [001] direction at 40K and 20K, This confirms the dominance of uniaxial magnetic anisotropy ($H_{2\perp} \gg H_{4\perp}$) in the sample.
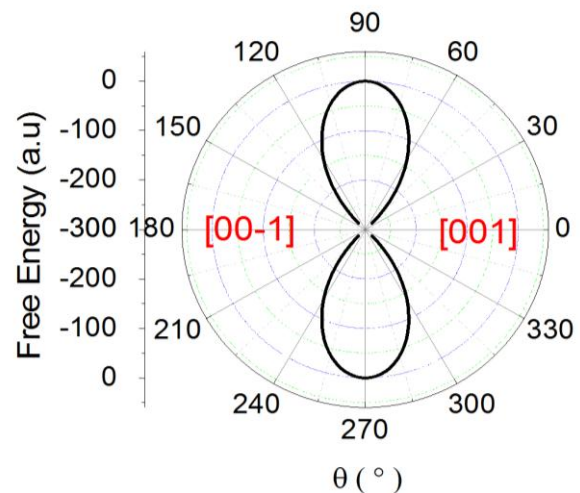

Fig. 6. 2D polar plot of free energy for the investigated sample at 40 K and 20 K, the plane contains 2 out-of-plane energy minima.

Conclusion

In this paper, measurements based on Hall Effect were performed on $Ga_{0.94}Mn_{0.06}As/In_{0.15}Ga_{0.85}As$ thin film to detect and control the magnetization orientations. At T = 5K, we evidenced a coexistence of both out-of-plane and in-plane magnetization components, with a net dominance of the in-plane component. With increasing temperature the out-of-plane magnetization component increases at the expense of the in-plane component. Analysis of magnetic anisotropy in this sample allows us to understand deeply the type of anisotropy as a function of temperature. At 5 K, the in-plane cubic anisotropy is dominance in the sample. At 20 K and 40 K out-of-plane uniaxial

anisotropy is formed. So that combining temperature condition and precise angular Hall effect measurements constitute a way to control the magnetic anisotropy in the DMS thin film. Further, this approach of controlling the rotating applied field constitutes a sensitive method for domain pinning fields in ferromagnetic single layers.

Author's contributions

MD conceived the experiments, prepared samples, carried out the experiments and data analysis. SK designed the experiments. RD assisted the experiments. JS carried out the molecular beam epitaxial growth. SC, TQH and FT supervise the work, M.D and TQH wrote the paper. The paper was revised by all the co-authors.

References

1. V. Novák, K. Olejník, J. Wunderlich, M. Cukr, K. Výborný, A. W. Rushforth, K. W. Edmonds, R. P. Campion, B. L. Gallagher, Jairo Sinova, and T. Jungwirth. *Phys. Rev. Let.*, **2008**, *101*, 077201.
   DOI: 10.1103/PhysRevLett.101.077201
2. Lin, C. Xiang. Y, Fuhua Y., Jianhua Z., Jennifer M., Peng X. and Stephan M. *Nano Lett.*, **2011**, *11*, 2584.
   DOI: 10.1021/nl201187m
3. X. Liu, Y. Sasaki, J.K. Furdyna, *Phys. Rev. B*, **2003**, *67*, 205204.
   DOI: 10.1103/PhysRevB.67.205204
4. Sunjae Chung, H. C. Kim, Sanghoon Lee, X. Liu, J. K. Furdyna, *Sol. Stat. Commun.*, **2009**, *149*, 1739.
   DOI: 10.1016/j.ssc.2009.07.024
5. Dietl, T. *J. Phys.: Condens. Matter.,* **2004**, *16*, S5471.
   DOI: 10.1088/0953-8984/16/48/001
6. A. Shen, H. Ohno, F. Matsukura, Y. Sugawara, N. Akiba, T. Kuroiwa, A. Oiwa, A. Endo, S. Katsumoto, Y. Iye, *J. Cryst. Growth*, **1997**, *175*, 1069.
   DOI: 10.1016/S0022-0248(96)00967-0
7. F. Matsukura, M. Sawicki, T. Dietl, D. Chiba, and H. Ohno, *Physica E*, **2004**, *21*, 1032.
   DOI: 10.1016/j.physe.2003.11.165
8. M. A. Herman and H. Sitter, Molecular Beam Epitaxy: Fundamentals and Current Status, Springer Series in Materials Science, Springer-Verlag, 2nd edition, **1997**.
9. P. Laukkanen, J. Sadowski, and M. Guina, Springer Series in Materials Science, Semiconductor researches: Experimental technique, Amalia Patane, Naci Balkan (Eds); *2012*, *1*, 150,
   DOI: 10.1007/978-3-642-23351-7
10. D. Chiba, M. Yamanouchi, F. Matsukura, T. Dietl, H. Ohno, *J. Magn. Magn. Mater.*, **2007***, 310*, 2078.
    DOI: 10.1016/j.jmmm.2006.10.1119
11. T. Dietl, H. Ohno, F. Matsukura, *Phys. Rev. B*, **2001**, *63*, 195205.
    DOI: 10.1103/PhysRevB.63.195205
12. M. Sawicki, F. Matsukura, A. Idziaszek, T. Dietl, G. M. Schott, C. Ruester, C. Gould, G. Karczewski, G. Schmidt, and L. W. Molenkamp, *Phys. Rev B*, **2004**, *70,* 245325.
    DOI: 10.1103/PhysRevB.70.245325
13. D. Chiba, M. Sawicki, Y. Nishitani, Y. Nakatani, F. Matsukura and H. Ohno, *Nature,* **2008**, *455*, 515.
    DOI: 10.1038/nature07318
14. W. Desrat, S. Kamara, F. Terki, S. Charar, J. Sadowski and D. K. Maude, *Semicond. Sci. Technol.*, **2009**, *24*, 065011.
    DOI: 10.1088/0268-1242/24/6/065011
15. J. Sadowski, J. Z. Domagala, J. Bak-Misiuk, S. Kolesnik, K. Swiatek, J. Kanskic, and L. Ilver, *Thin. Solid. Films.*, **2000**, *367*, 165.
    DOI: Structural properties of MBE grown GaMnAs layers
16. P.A. Bone, J.M. Ripalda, G.R. Bell, T.S. Jones, *Surf. Sci.*, **2006**, *600*, 973.
    DOI: 10.1016/j.susc.2005.12.015
17. A. Wolska, K. Lawniczak-Jablonska, M.T. Klepka, R. Jakieła, I.N. Demchenko, J. Sadowski, E. Holub-Krappe, A. Persson and D. Arvanitis, *Acta. Phys. Pol. A.*, **2008**, *114*. 357.
    DOI: 10.12693/APhysPolA.114.357
18. J. Sadowski, R. Mathieu, P. Svedlindh, J. Z. Domagala, J. Bak – Misiuk, K. Swiatek, M. Karlsteen, J. Kanski, L. Ilver, H. Åsklund, U. Södervall, *Appl. Phys. Lett.*, **2001**, *78*, 3271.
    DOI: 10.1063/1.1370535
19. S. Adachi, Physical Properties of III-V Semiconductor Compounds: InP, InAs, GaAs, GaP, InGaAs and InGaAsP, Wiley-VCH Verlag, **1992**.
20. J. Masek, J. Kudrnovsky, and F. Maca, *Phys. Rev. B*, **2003**, *67*, 153203.
    DOI: 10.1103/PhysRevB.67.153203
21. J. Sadowski, J. Z. Domagała, *Phys. Rev. B*, **2004**, *69*, 075206.
    DOI: 10.1103/PhysRevB.69.075206
22. Nakagawa. S, Sasaki. I and Naoe. M. *J. Appl. Phys.*, **2002**, *91*, 8354.
    DOI: 10.1063/1.1456418
23. K. Okamoto, *J. Magn. Magn. Mater.*, **1983***, 35*, 353.
    DOI: 10.1016/0304-8853(83)90539-5
24. Son H, Chung S J, Yea S Y, Lee S, Liu X and Furdyna J. K, *J. Appl. Phys.*, **2008**, *103*, 07F313.
    DOI: 10.1063/1.2834448
25. D. G. Stinson, A. C. Palumbo, B. Brandt and M. Berger, *J. Appl. Phys.*, **1987**, *61*, 3816.
    DOI: 10.1063/1.338606
26. Shinhee Kim, Hakjoon Lee, Taehee Yoo, Sangyeop Lee, Sanghoon Lee, X. Liu and J. K. Furdyna, *J. Appl. Phys.*, **2010**, *107,* 103911.
    DOI: 10.1063/1.3427553
27. Lee, H., Chung, S., Lee, S., Liu, X. and Furdyna, J. K., *Solid. State. Commun.*, **2009**, *149*, 1300.
    DOI: 10.1016/j.ssc.2009.05.006
28. Sanghoon Lee, Taehee Yoo, Hakjoon Lee, Sungwon Khym, Xinyu Liu and Jacek K. Furdyna. *Jpn. J. Appl. Phys.*, **2011***, 50*, 04DM02.
    DOI: 10.1143/JJAP.50.04DM02
29. Y. Zhai, Y. X. Xu, J. G. Long, Y. B. Xu, M. Lu, Z. H. Lu, H. R. Zhai, and J. A. C. Bland, *J. Appl. Phys.*, **2001**, *89*, 7290.
    DOI: 10.1063/1.1359458